ESD-TR-91-250

(2)

Technical Report
950

Geometrical Transformation of Linear Diode-Laser Arrays for Longitudinal Pumping of Solid-State Lasers

J.R. Leger
W.C. Goltsos

26 May 1992

Lincoln Laboratory
MASSACHUSETTS INSTITUTE OF TECHNOLOGY
LEXINGTON, MASSACHUSETTS

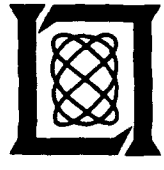

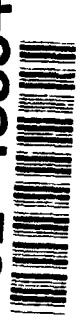

Prepared for the Defense Advanced Research Projects Agency
under Air Force Contract F19628-90-C-0002.

This report is based on studies performed at Lincoln Laboratory, a center for research operated by Massachusetts Institute of Technology. The work was sponsored by the Defense Advanced Research Projects Agency under Air Force Contract F19628-90-C-0002.

The ESD Public Affairs Office has reviewed this report, and it is releasable to the National Technical Information Service, where it will be available to the general public, including foreign nationals.

This technical report has been reviewed and is approved for publication.

FOR THE COMMANDER

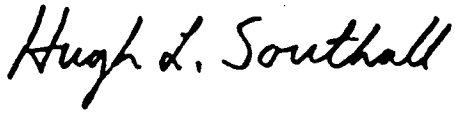

Hugh L. Southall, Lt. Col., USAF
Chief, ESD Lincoln Laboratory Project Office

Non-Lincoln Recipients

PLEASE DO NOT RETURN

Permission is given to destroy this document when it is no longer needed.

MASSACHUSETTS INSTITUTE OF TECHNOLOGY
LINCOLN LABORATORY

GEOMETRICAL TRANSFORMATION OF LINEAR DIODE-LASER ARRAYS FOR LONGITUDINAL PUMPING OF SOLID-STATE LASERS

J.R. LEGER
W.C. GOLTSOS
Group 52

TECHNICAL REPORT 950

26 MAY 1992

LEXINGTON MASSACHUSETTS

ABSTRACT

A 200-stripe linear diode-laser array is geometrically transformed into a two-dimensional, symmetric virtual source with symmetric divergence to end-pump a Nd:YAG laser. The geometrical transformation is performed by two planes of diffractive optical elements separated by a 2.6-cm gap. Discounting optical losses, a TEM_{00}-mode slope efficiency of 56 percent is demonstrated. Methods of increasing the throughput efficiency of the diffractive elements (currently approximately 50 percent per element) are explored. A theoretical model for estimating the maximum useful pump array size in longitudinally pumped rod and fiber lasers shows that this pump geometry is close to optimum.

ACKNOWLEDGMENTS

We gratefully acknowledge the program managers L. Durvasula of the DARPA Defense Science Office and N. Pchelkin of the Air Force Phillips Laboratory. Their support, through the eye protection and the pilot programs, pave the way for the layered and off-axis microoptics technology described in this report. They steadily encouraged a long-term view in the development of unconventional and composite microoptics structures for use in layered imaging systems and coupled microlaser cavities.

We thank William Delaney and Marsden Griswold for fabricating the diffractive microlens arrays discussed in this report. This project benefited from numerous interactions with Gary Swanson. Wilfred Veldkamp is the program manager.

TABLE OF CONTENTS

LIST OF ILLUSTRATIONS

1. INTRODUCTION

Diode-laser arrays are ideal illumination sources for a variety of applications. They can be fabricated with high electrical-to-optical efficiencies; they have demonstrated very high reliability. Large laser arrays can produce hundreds of watts of optical power. Their narrow spectrum makes them ideally suited to pumping solid state and fiber lasers.

There are two principal drawbacks to diode-laser arrays for pumping applications. The first drawback is that the lasers in the array are essentially mutually incoherent. The radiance theorem therefore sets a theoretical limit on one's ability to focus the light into a desired volume. The second drawback arises from the linear geometry of most diode-laser arrays. The resulting line source is not well matched to applications such as longitudinal pumping. Most high-power pumping applications have had to employ less efficient transverse and slab pumping geometries.

This report describes an optical device that converts a one-dimensional diode-laser array into a two-dimensional light field capable of longitudinally pumping a solid-state laser in an optimal manner. The radiance theorem is reviewed and used to calculate an optimum pumping geometry. Limits to longitudinal pumping of both rod and fiber lasers are explored. A description of the effects of the various imaging systems on radiance is included, showing that microoptics can achieve the desired geometry.

The design and fabrication of a specific optical device is described next, including a discussion on how the design is capable of producing a pump radiance that is limited only by the radiance theorem. The optical and mechanical tolerances are considered, as well as ways of relaxing them. Fabrication of the required optics and the theoretical efficiency are then discussed. Longitudinal pumping of an Nd:YAG laser is demonstrated with these optics and a 1-cm wide diode-laser array. Pump characteristics and laser performance are reported. Next, the laser performance is analyzed with a detailed computer model. Finally, the experimental results are compared with theory; the performance of the design is compared to other longitudinal pumping schemes.

2. THEORY OF OPTIMAL PUMP GEOMETRIES

The light produced by an optical source can be characterized in a variety of ways, with the overall power being the most common. Although this is appropriate for some applications, it does not describe any of the focusing properties of the array. Efficient longitudinal pumping of a volume imposes additional constraints on the source. The power must be deposited in a small region of space, and the divergence must be minimized so the pump cross-sectional area stays small throughout the volume of interest. Similar constraints occur when coupling light into a waveguide such as a multimode fiber [1], where both the spot size and numerical aperture of the pump must be less than or equal to the entrance aperture and numerical aperture of the guide. For these applications, the radiance $B(x, y, \theta_x, \theta_y)$ (power per unit area per unit solid angle) is the most meaningful pump characteristic.

2.1 Radiance Theorems

There are two important theorems that govern radiance in an optical system. The first, called the radiance theorem [2], states that the radiance of the light distribution produced by an imaging system cannot be greater than the original source radiance (assuming that both object and image spaces have the same index of refraction); the radiances are equal only when the losses in the optics are negligible. The second related theorem states that the radiance of a collection of mutually incoherent (but otherwise identical) sources cannot be increased by a passive linear optical system to a level greater than the radiance of the single brightest source. These two theorems imply that there is a theoretical limit to the radiance of the pump light. Optimum pumping optics must match the spatial and angular characteristics of the pump to the laser mode, subject to this radiance limit.

It is instructive to calculate the radiance of a single spatial mode source. If the lowest-order mode from a diode laser is approximated as a Gaussian with a lateral waist of ω_x and a transverse waist of ω_y ($1/e^2$ intensity point), then the divergence in the x direction is given by

$$\theta_x = \frac{\lambda}{\pi \omega_x}, \tag{1}$$

where λ is the wavelength of light. The divergence in the y direction is given by a similar equation. The radiance $B(x, y, \theta_x, \theta_y)$ is nonnegligible over a four-dimensional volume, E_p, approximated by the product of the aperture area and its solid-angle divergence. This product is known as the étendue of the beam. Using the small angle approximation, the étendue of a Gaussian beam is

$$E_p = \lambda^2. \tag{2}$$

The resulting radiance (centered and on-axis) is given by

$$B(0,0,0,0) = \frac{4P}{\lambda^2}, \tag{3}$$

where P is the total power. Note that the étendue and radiance are independent of the size and divergence of the source. This is as expected, because a lossless magnification cannot change the radiance.

The factor of 4 in Equation (3) comes from the fact that the radiance is not uniformly distributed throughout the volume E_p but peaks in the center. It is often more convenient to define the average radiance B' simply as the power divided by the étendue. For a two-dimensional Gaussian beam,

$$B' = \frac{P}{\lambda^2}. \tag{4}$$

There are certain cases where the radiance of a multilaser pump source can exceed the radiance of the individual elements. First, if mutual coherence is established across the pump lasers [3,4], the entire source behaves as a single-spatial mode, and the phase and amplitude can in principle be made uniform. Adding additional *mutually coherent* lasers to the array does increase the radiance, and the resulting total radiance can be equal to the sum of the individual laser radiances.

A second way to increase radiance is to use pump lasers with different average properties (such as wavelength or polarization). Passive optical elements such as diffraction gratings and polarizing beam splitters can be used to multiplex the beams.

For this report assume that the pump array consists of polarized, mutually incoherent,[1] single spatial-mode sources with identical wavelengths and, therefore, the radiance theorem and its corollaries can be directly applied to each polarization state.

2.2 Pumping Limits

The étendue of a source measures the approximate volume of four-dimensional radiance space containing significant radiance. Mutually incoherent sources of the same polarization must occupy unique volumes in radiance space. Overlap of these volumes would require an increase in radiance that is forbidden by the second radiance theorem. It now becomes a simple matter to calculate the maximum number of mutually incoherent pump lasers that can be used in a particular pumping configuration. Counting both polarizations, the total number of pump beams N is simply given by

[1] At low powers, some closely spaced arrays exhibit varying degrees of spatial coherence. In principle, this coherence can be utilized to increase the number of pump beams coupled into the laser mode. The coherence is usually reduced at high powers, however, and will not be exploited here.

$$N = 2\frac{E_l}{E_p}, \tag{5}$$

where E_l is the étendue of the element to be pumped, and E_p is the minimum étendue of a single-mode source.

As a first example, the number of mutually incoherent Gaussian pump beams that can be coupled into a multimode fiber with core radius a and numerical aperture (NA) is calculated. The fiber étendue E_l is given by

$$E_l = \pi^2 a^2 (NA)^2, \tag{6}$$

where the small angle approximation is used to calculate the solid angle. Because the étendue of a Gaussian beam is λ_p^2 where λ_p is the pump wavelength, the total number of pump beams N is given by

$$N = 2\frac{\pi^2 a^2 (NA)^2}{\lambda_p^2} = \frac{V_p^2}{2}, \tag{7}$$

where V_p is the V-number of the fiber at the pump wavelength given by

$$V_p = \frac{2\pi a (NA)}{\lambda_p}. \tag{8}$$

Note that N is simply equal to the number of modes supported by the multimode fiber [5].

To analyze a single-mode fiber laser with a simple single cladding, Equation (7) can be rewritten in terms of the core V-number V_l at the lasing wavelength λ_l. Because $V_p = (\lambda_l/\lambda_p)V_l$,

$$N = \frac{V_l^2}{2}\left(\frac{\lambda_l}{\lambda_p}\right)^2. \tag{9}$$

A single-mode fiber [5] must have a V-number $V_l < 2.405$, limiting the maximum number of pump beams to

$$N < 2.89\left(\frac{\lambda_l}{\lambda_p}\right)^2. \tag{10}$$

For a simple Nd:Glass fiber laser pumped at 0.8 μm, the maximum value of N is approximately 5.

The number of pump beams can be increased by using a fiber laser with two claddings [6]. The laser light in the single-mode core is guided by the inner cladding. A second outer cladding is introduced to guide light from the inner cladding, effectively making a multimode waveguide. The pump beams can thus be distributed throughout the inner cladding with the guided pump light being slowly absorbed by the doped core. Double-clad structures can be pumped with, at most, $V_p^2/2$ lasers, where V_p is the V-number of the first cladding guided by the second. For one particular double-clad fiber laser [7] with a 45 x 110 μm rectangular inner cladding and $NA = 0.4$, the theoretical number of pump beams is 7,775. Considering 65 mW per pump beam, this represents over 500 W of pump power injected into the fiber laser.

The number of pump beams that can be coupled into a laser rod can be determined by calculating the étendue of the laser mode over a fixed length. A simple approximate expression can be obtained by referring to Figure 1. The laser mode has a waist of ω_l; a crystal length L is chosen to absorb the majority of the pump beam. The divergence of the laser mode is assumed to be small so that diffraction within the crystal is negligible. The pump-beam waist ω_{p_0} is assumed to be small when it is compared to ω_l; therefore, the number of pump beams is large. An area and solid angle are sought that will completely contain the parallel propagating pump beams within the laser mode throughout the crystal. The figure shows that pump beams can be placed out a distance R from the center and can still be contained within the laser mode as long as

$$R \leq \omega_l - \omega_p(L/2), \tag{11}$$

where $\omega_p(L/2)$ is the spot size of the pump beam at the end of the crystal. Because ω_{p_0} is small,

$$\omega_p(L/2) \approx \frac{\lambda_{eff} L}{2\pi\omega_{p_0}}, \tag{12}$$

where λ_{eff} is the effective wavelength of the pump light in the laser rod. The area of the region described by Equation (11) is given by

$$\pi R^2 = \pi\left(\omega_l - \frac{\lambda_{eff} L}{2\pi\omega_{p_0}}\right)^2. \tag{13}$$

The solid-angle divergence (using a small angle approximation) from a pump beam of waist ω_{p_0} is given by

$$\Omega = \frac{\lambda_{eff}^2}{\pi\omega_{p_0}^2}, \tag{14}$$

resulting in a laser étendue E_l of

$$E_l = \left(\omega_l - \frac{\lambda_{eff} L}{2\pi\omega_{p0}}\right)^2 \frac{\lambda_{eff}^2}{\omega_{p0}^2}. \tag{15}$$

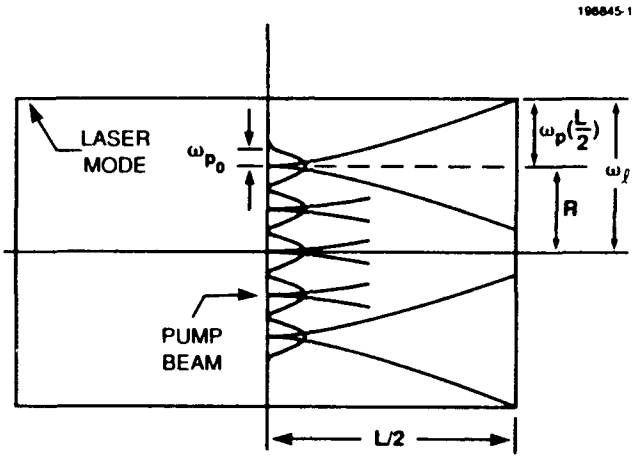

Figure 1. Calculating the étendue of an end-pumped rod laser. Parallel-propagating pump beams are shown inside the pump volume.

It is easy to show that E_l is maximized when

$$\omega_{p0} = \frac{\lambda_{eff} L}{\pi\omega_l}, \tag{16}$$

resulting in a maximum étendue of

$$E_l = \frac{\pi^2\omega_l^4}{4L^2}. \tag{17}$$

Because the étendue of a single Gaussian pump beam $E_p = \lambda_{eff}^2$, the maximum number of mutually incoherent pump beams N that can be packed into the laser pump volume (volume of the laser mode where the pump light is absorbed) is given by

$$N = \frac{\pi^2 n^2 \omega_l^4}{2L^2 \lambda_p^2} \, , \; N \gg 1 \tag{18}$$

where the free-space wavelength of the pump light $\lambda_p = \lambda_{eff}/n$ has been substituted, with n = refractive index of the laser rod. Note that the number of mutually incoherent pump beams increases as the fourth power of the laser mode waist. This indicates that end pumping is inherently scalable if the pump volume is utilized efficiently [8]. The number of pump beams increases as the absorption coefficient increases (resulting in a smaller crystal length L).

Equation (18) is accurate only for large N. The equation for small N as L approaches infinity is given by dividing the étendue of the laser mode itself by the étendue of a pump beam:

$$N = 2\left(\frac{\lambda_l}{\lambda_p}\right)^2 \, , \; N \sim 1 \tag{19}$$

where λ_l is the free-space wavelength of the laser light and $\lambda_l > \lambda_p$.

3. DESIGN OF OPTICAL SYSTEMS FOR OPTIMUM PUMPING

Section 2 described the conditions for optimum pumping. This section reviews the optical requirements for achieving optimal pumping and describes the effect of several optical systems. A specific optical design is presented that implements all of these requirements.

3.1 Optical Requirements

The étendue E_p of Equation (2) is for a diffraction-limited Gaussian beam. Aberrations in the pump beam can significantly reduce the beam radiance and result in coupling fewer pump beams into the laser pump volume. The first requirement is to convert each single-spatial-mode pump into a diffraction-limited distribution with minimum étendue. Astigmatism is a common aberration prevalent in gain-guided lasers. The astigmatic wavefront cannot be collimated with a circularly symmetric lens. A properly designed optical system must contain an anamorphic collimating lens to remove this aberration. Other aberrations should be removed in a similar manner.

The second requirement is to pack the pump modes in radiance space so that there is no wasted space between modes. Typical CW arrays contain significant inactive regions to reduce the heat load. A simplified linear diode-laser pump source is shown in Figure 2(a) that consists of emitting apertures spaced by large dark regions. Figure 2(b) shows a two-dimensional slice through radiance space along the x and θ_x axes. Each pump beam radiates into the same angular cone, but the radiating apertures are separated by substantial inactive regions. The extent of the laser étendue is shown as a dotted line, where the integrated power falling in this region contributes to the laser mode. Because the divergence of the beams is large, only about one-third of each pump beam falls within this dotted region.

The effect of various optical systems on the pump distribution can be displayed in the $x - \theta_x$ diagram. The divergence of the pump beams can be reduced by the magnification system shown in Figure 2(c), but the spatial separation is increased. Figure 2(d) shows that a single-pump beam is now completely contained within the laser étendue. The other two beams are imaged outside the region of interest, however, and the pumping power contributing to the laser mode is roughly the same. Note that the total area containing substantial pump radiance in Figure 2(d) is unchanged (as required by the radiance theorem) and that the overall area required to contain all the pump beams is also unchanged.

Figure 2(e) shows a focusing system where the pump array has been placed in the front focal plane of the lens, and the light is observed in the back focal plane. The pump beams now occupy a common area but are incident at different angles. The roles of space and angle have been reversed, and the effect shown in Figure 2(f) is simply to rotate the diagram in Figure 2(b) by 90 deg. As in the previous case, only a single-pump beam contributes to the laser mode, and the useful pump power is unchanged. Again, the pump area in the diagram is preserved, and the dark spaces between pump beams have not been removed.

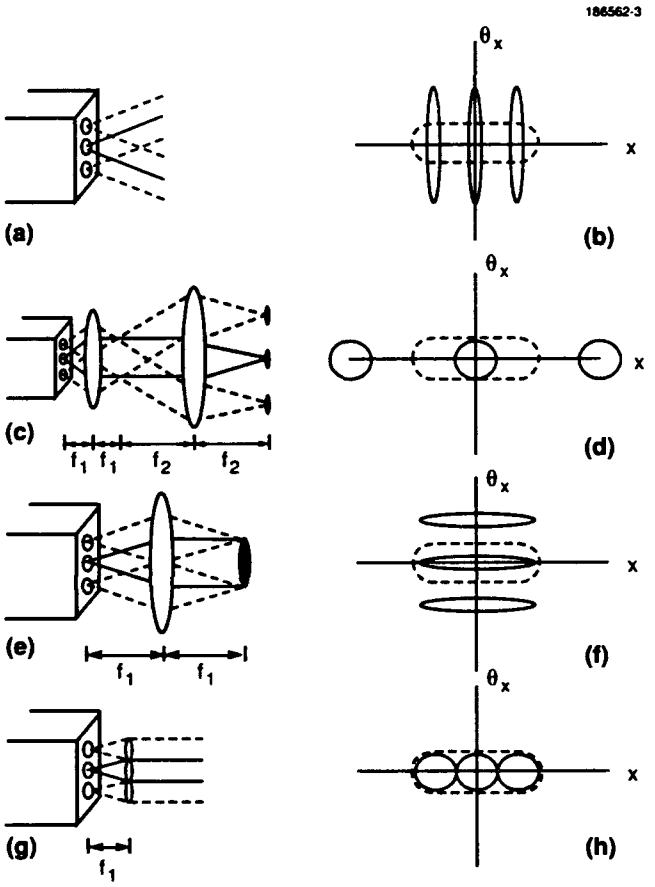

Figure 2. Effect of coupling optics on power distribution in radiance space. (a) and (b) show distribution with no coupling. (c) and (d) show the effect of optical magnification. (e) and (f) show the effect of focusing optics. (g) and (h) show the effect of individual microoptic collimating lenses.

The third optical system shown in Figure 2(g) contains collimating microoptics. Each pump beam is allowed to expand to an optimal size and is then individually collimated. The effect is to perform the magnification illustrated in Figures 2(c) and (d) on each beam independently. An increase in beam size to cover the gaps between beams is accompanied by a decrease in divergence. The overall spacing of the pump beams, however, does not change. Figure 2(h) shows that this optical system has densely packed three complete pump beams within the laser étendue. Note that the total area containing light in the figure is still unchanged, but the area required to contain all the beams is reduced. Both macroscopic [9] and microscopic [10] versions of these aperture filling optics have been applied previously to diode-laser arrays.

The third requirement for optimal pumping is to place pump beams throughout the four-dimensional laser étendue. This corresponds to fully utilizing the spatial and angular extent of the laser pump volume. Figure 3 illustrates the amount of radiance space used by a linear diode-laser array with conventional imaging. A different two-dimensional slice through radiance space containing the x and y axes is shown in Figure 3(a), and a corresponding slice containing the θ_x and θ_y axes is shown in Figure 3(b). The extent of the laser étendue is again shown as a dotted line. Note that longitudinal pumping of a conventional resonator mode leads to a laser étendue that is circularly symmetric in both space and divergence. A geometric transformation is required to convert the pump distribution in Figure 3(a) into the ideal symmetric distribution shown in Figure 3(c). The asymmetric divergence in Figure 3(b) can be converted into the required symmetric divergence of Figure 3(d) by anamorphic imaging.

3.2 Design of a Specific Optimal Pumping System

Optimal pumping optics have been designed for a linear CW diode-laser array fabricated by Spectra Diode Labs (SDL3480). This array consists of 200 pump lasers contained in 20 subarrays. The 10-laser waveguides in each subarray are 6 μm wide on 10 μm centers, resulting in a total subarray length of close to 100 μm. The spacing of the subarrays is 500 μm, for a total array length of approximately 1 cm.

Previous interferometric measurements [10] on similar gain-guided lasers showed significant astigmatism. The wavefront transverse to the junction is essentially flat at the aperture, whereas the wavefront parallel to the junction appears to be emanating from a point source 20 μm inside the waveguide. The divergence is approximately 40 deg (full-width at half-maximum) transverse to the junction and 10 deg parallel to the junction. The total power of the array is approximately 5 W.

The pumping optics were designed to meet all the requirements outlined in the previous section. In order to take advantage of polarization multiplexing, two identical optical systems were designed to operate on the left and right half of the array in parallel. The outputs of these two systems were then multiplexed using a half-wave plate and polarizing beam splitter. The following describes one of these optical systems applied to half the pump array (100 lasers).

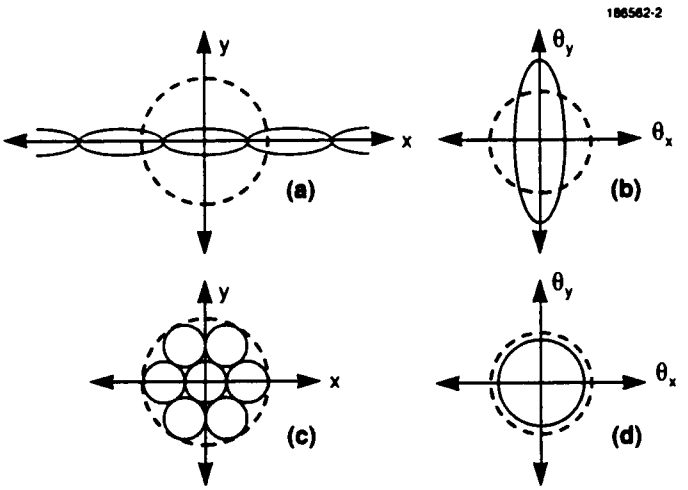

Figure 3. Distribution of power in space and angle. (a) shows the spatial distribution of a linear pump source, (b) shows its divergence, (c) illustrates the advantages of converting the one-dimensional source to a two-dimensional virtual array, and (d) shows the proper divergence has been achieved by symmetrizing the pump beams and optimizing the beam waists.

The nonsymmetric divergence is a result of diffraction from the noncircular diode-laser aperture. The divergence was symmetrized by using an anamorphic imaging system (see Figure 4). The light was collimated in the transverse direction by the cylindrical lens ℓ_{y1} shown in Figure 4(a) with a focal length f_{y1} = 500 μm and a numerical aperture of 0.45. The front facet of the laser aperture was placed in the front focal plane of this lens, resulting in a collimated transverse beam diameter of approximately 500 μm. In the lateral direction, a pair of cylindrical lenses ℓ_{x1} and ℓ_{x2} was used in an afocal configuration to image an entire subarray of 10 lasers with a magnification of 50× [see Figure 4(b)]. The magnified subarray contained images of the laser apertures spaced in the lateral direction by 500 μm, with the lateral image of each laser aperture slightly less than 500 μm. The two crossed cylindrical lenses ℓ_{x1} and ℓ_{y1} were designed to be placed in the same plane. The astigmatism of the gain-guided laser was removed by selecting the focal length of ℓ_{x1} (f_{x1} = 509.8 μm) to place its object plane 20 μm in front of the laser facet. The resulting image plane was 26.0 mm behind the lens. The focal length of lens ℓ_{x2} (f_{x2} = 25.49 mm) was then selected to cancel the phase curvature in the lateral image plane. The curvature in the transverse direction resulting from diffraction was negligible and was not corrected. The combined effect of the lateral and transverse imaging systems produced an array of 10 spots, each with a roughly symmetric aperture (and therefore symmetric divergence).

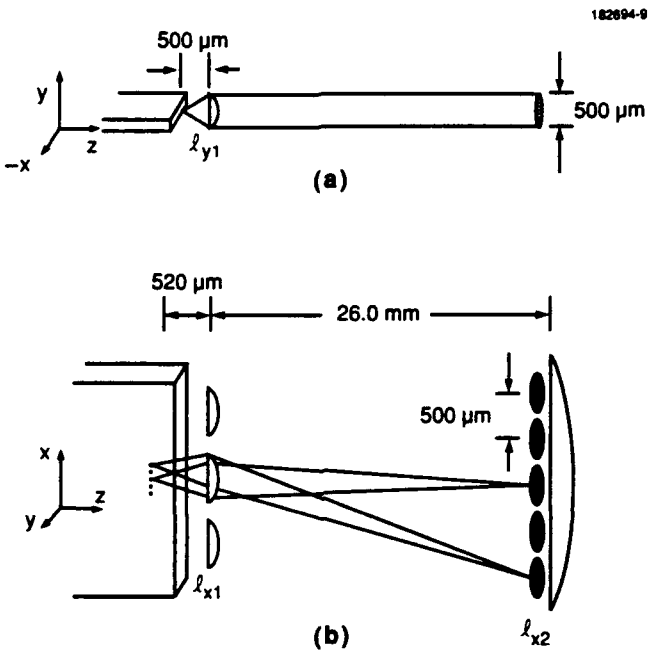

Figure 4. Imaging optics in the transverse and lateral directions. (a) shows a cylindrical lens to collimate the beam in the transverse direction. (b) shows an afocal magnification system (50×) in the lateral direction. The resultant pump beams are approximately circular and are indicated by the shaded areas.

Aperture filling and geometric transformation were performed by using prismatic optics to direct the different laser beams into a two-dimensional geometry. The first set of prisms was placed in the same plane as lenses ℓ_{x1} and ℓ_{y1}. The images from each 10-laser subarray were redirected by prisms to overlap in the lateral direction [Figure 5(a)]. At the same time, the images were deflected in the transverse direction by an orthogonal set of prisms to form 10 separate rows of lasers separated by 500 μm each [Figure 5(b)]. The resulting two-dimensional array of 10×10 lasers formed a square 5 mm on each side. A second set of prismatic optics was required in the ℓ_{x2} lens plane to correct for the image tilts and redirect all the beams along the optical axis.

The entire optical system is shown pictorially in Figure 6 operating on one-half of the pump array. Only 7 of the 10 subarrays are shown for clarity. An identical optical system was registered to the other half of the array to form a second 10×10 array, 5 mm away. The two square arrays thus abutted one another with no gaps.

Note that all the optics described above are contained in two planes. An additional lens is shown in Figure 6 to match the size or divergence requirements of a specific laser system. This lensing function can, in principle, be incorporated into the second plane of optics. However, the

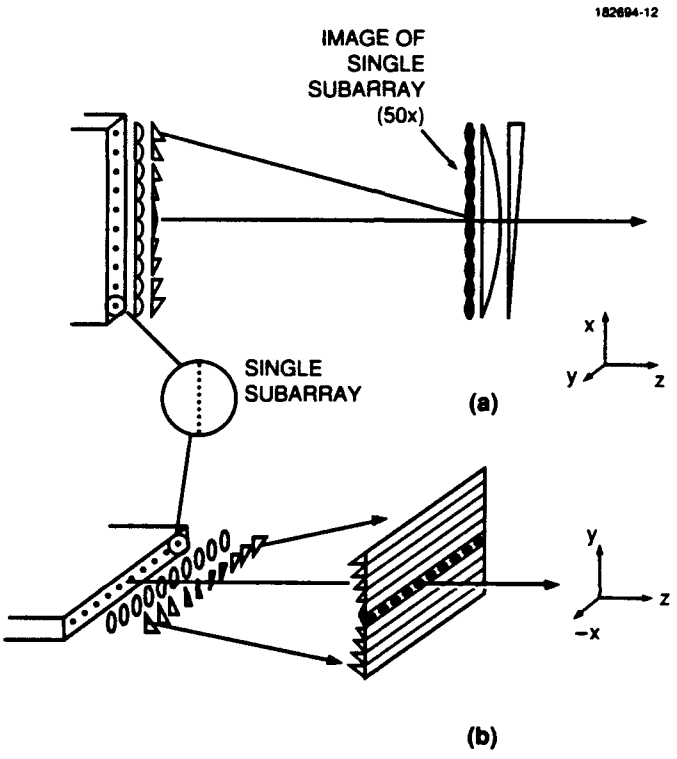

Figure 5. Geometrical transformation using an array of prisms. In (a), different prisms are applied to each subarray to steer the images laterally to a common location. Prisms (one shown) are placed in the second plane of optics to remove the tilts introduced by the first plane. The transverse beam steering shown in (b) is accomplished by an additional set of prisms to form a two-dimensional array. These tilts are removed by a complementary set of prisms in the second plane.

external configuration shown permits the same front-end optical system to be used for a variety of applications simply by adjusting the focal length of the external lens.

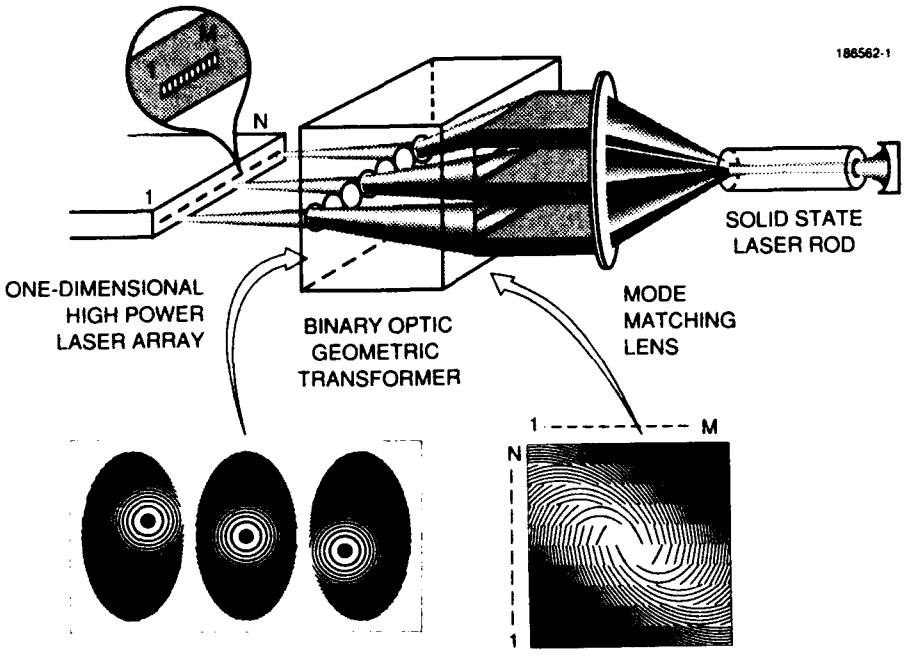

Figure 6. Optical implementation using diffractive optics (binary optics). All lens and prism functions are performed by two planes of surface-relief optics. The mode-matching lens is selected to match the laser mode. Only seven of the 10 subarrays and lenslets are shown for clarity. The lower insets show representative phase patterns for the lenslets of the first and second planes of optics.

3.3 Mechanical Tolerances

The tolerance to positional errors is of great practical importance. Errors can result from inadequate mounting, as well as from positional variations in the pump array. The longitudinal (focus) tolerance is strictly governed by the numerical aperture of the pump array and follows the same rules as any collimating optic. Specifically, the longitudinal tolerance Δz is given by

$$\Delta z = \pm \frac{\lambda}{2(NA)^2}. \tag{20}$$

For the present design, the numerical aperture in the transverse direction is 0.45, making the longitudinal tolerance approximately ± 2 wavelengths, or a total longitudinal tolerance of 3.2 μm for a pump wavelength of 0.8 μm. Of course, this tolerance can be relaxed if there are fewer pump beams than the theoretical maximum given by Equations (7) or (18). In this case, diffraction-limited performance is not required and some amount of misfocus aberration can be tolerated.

In the lateral direction, the optics form a magnified image. It is clear that a shift of one laser spacing in the object produces a shift of one laser spacing in the image. In our case, mispositioning the pump beams by 10 μm in the lateral direction shifts all of the lasers by one laser spacing, with one column (10 percent of the lasers) shifted off the second set of lenses. However, if these lenses are made oversized in the lateral direction, the only effect is to shift the entire pump beam by 10 percent of its width. This can be compensated by adjusting the resonator mirrors to reposition the laser mode. In addition, if the number of pump beams N is smaller than the theoretical maximum, this tolerance can be significantly relaxed.

Misplacement by an amount h transverse to the junction causes the collimated beams exiting the first set of optics to have an excess transverse tilt. After propagating to the second plane of optics, the displacement x in the second plane is related to the shift in the first plane by

$$h = \frac{f_{y1}}{z} x, \tag{21}$$

where z is the separation between the two planes of optics and f_{y1} is the transverse focal length of the first lens. This displacement must be kept much smaller than the lens spacing in the second plane of optics. In the optical design, $f_{y1} = 500$ μm, $z = 2.6$ cm, and the lens spacing in the second plane is 500 μm. Thus, $x \ll 500$ μm is required and the displacement h must be much smaller than 9.6 μm. Unlike the lateral displacement error, the laser mode cannot be shifted to correct for the transverse shift error because the misdirected beams illuminate the wrong lenses in the second plane of optics and are redirected out of the desired pump region entirely. In this case, a mispositioning of the entire array by 0.96 μm reduces the coupled power by 10 percent. If a looser tolerance is required, the optical system can be modified by increasing the transverse width of the second lens set to underfill each lens. For example, if each lens width in the above case is doubled, shifts in the second plane up to $x = 500$ μm can be compensated by a simple readjustment of the laser mode position. This corresponds to a transverse pump displacement tolerance of $h < 9.6$ μm. The penalty paid for this increased tolerance is a loss of fill factor (in this case by 50 percent), and hence the maximum number of pumps possible is reduced.

4. IMPLEMENTATION OF OPTICAL SYSTEM USING BINARY OPTICS

The optical design of Section 3.2 was described in terms of cylindrical lenses and prisms. The optical phase function $\phi_n(x,y)$ that combines all the elements in the first plane is given by

$$\phi_n(x,y) = \frac{2\pi}{\lambda}\left[\sqrt{f_{y1}^2 + x^2 + y^2} + \frac{x^2}{2f'} + \sin(\theta_{xn})x + \sin(\theta_{y_n})y\right], \tag{22}$$

$$\text{where } f' = \frac{f_{y1}f_{x1}}{f_{y1} - f_{x1}},$$

and the subscript ϕ_n corresponds to the optical element applied to the nth laser subarray. The square root term represents an aspheric (but circularly symmetric) imaging lens and the additional quadratic term makes the system anamorphic. The last two terms represent prisms, where the lateral and transverse angles θ_{xn} and θ_{y_n} are chosen to steer the individual subarrays into a two-dimensional pattern. The second plane of lenses can be described in a similar manner.

Equation (22) describes a highly aspheric surface. Both planes of optics contain 20 aspheric elements (two groups of 10) with each element separated by 500 μm. The two planes are fabricated as diffractive optical elements. Integer numbers of wavelengths are subtracted from the phase function $\phi_n(x,y)$ to create a discontinuous phase contour between 0 and 2π radians. This modified phase function is then quantized into discrete levels, and microlithography and dry etching are used to transfer the phase pattern into a surface relief structure [10]. Representative examples of the phase patterns for the lenslets in the first and second planes of optics are shown as insets in Figure 6.

The number of phase levels affects the efficiency of the optical elements. Eight phase levels are fabricated in three etching steps. In the scalar theory limit (features large compared to a wavelength), eight phase levels should result in a diffraction efficiency of about 95 percent [10]. However, high-numerical-aperture diffractive lenses usually do not achieve this efficiency because the features at the edge of the lens become comparable to the optical wavelength. The actual efficiency computed by vector diffraction theory is both a function of the lens numerical aperture and the substrate refractive index [11].

The chromatic dispersion of the elements is an additional potential source of error. Because the elements are diffractive, the focal length shifts with wavelength according to

$$\Delta f = -f\frac{\Delta\lambda}{\lambda}. \tag{23}$$

Substituting the allowable longitudinal shift given in Equation (20) for Δf and solving for $\Delta\lambda$ gives

$$\Delta\lambda = \pm\frac{\lambda^2}{2f(NA)^2}. \tag{24}$$

For this experiment, $\lambda = 0.8$ μm, $f = 500$ μm, and $NA = 0.45$. The allowable wavelength shift is then ± 3.2 nm. Because the spectral width of the diode-laser array is 3 nm (full-width at half-maximum), the chromatic dispersion does not present a problem.

5. EXPERIMENTAL SETUP

As an initial demonstration of the geometric transformation concept, an Nd:YAG laser will be longitudinally pumped with the 5-W CW linear diode-laser array (SDL3480). The array was mounted onto a thermoelectric cooler to permit temperature tuning of the emission wavelength to match the peak absorption of the Nd:YAG crystal. The first optical element of the transformation system, consisting of a linear array of off-axis anamorphic lenslets described by Equation (22), was positioned in front of the pump array by a Photon Control INFOLD six-axis micromanipulator. All rotations of the optical element occurred about a single point in space coinciding with the center of the component. Fine positioning was provided by piezoelectric translators to achieve the tolerances computed in Section 3.3. The second optical element was mounted in a four-axis manipulator. Alignment of this component was less critical and rotation was provided only about the optic axis. The output of this element consisted of two symmetric, geometrically transformed beams.

The effective source radiance was increased by polarization multiplexing the two symmetric beams as shown in Figure 7. One beam was deflected to pass through a polarization rotator and then combined with the undeflected beam in a polarizing beamsplitter. The combined beam was focused approximately 2 mm beyond the facet of the 1.1 percent-doped Nd:YAG crystal with a 38.1-mm focal-length mode-matching lens for highest laser output power (see Section 7 , Figures 13 and 14). The two ends of the 1-cm-long, 3-mm-diameter Nd:YAG crystal were polished flat and parallel and had a dichroic coating on the pump end and an antireflection coating at 1.06 μm on the resonator end. Residual reflectivity from the crystal face at 808 nm was 1.5 percent. The output coupler of the plano-concave resonator had a 50-cm radius of curvature and was 5 percent transmitting at the laser wavelength. The overall resonator length of 37 mm resulted in a TEM_{00} mode size of 210 μm.

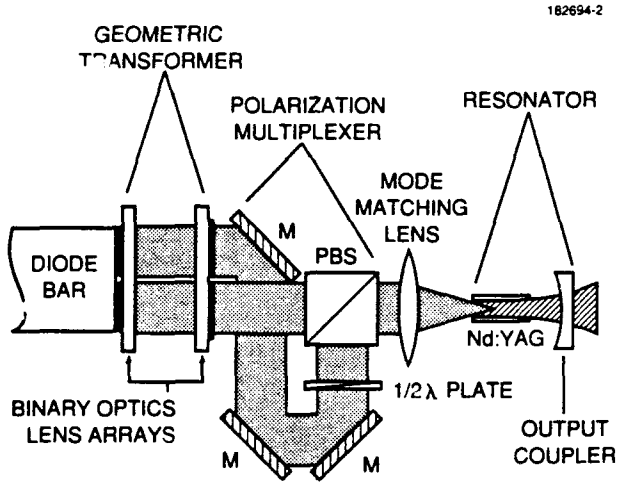

Figure 7. Schematic diagram of experimental setup showing polarization multiplexing and focusing optics, and Nd:YAG resonator. PBS=Polarizing Beam Splitter, M=Mirror.

6. EXPERIMENTAL RESULTS

The photographs of Figure 8 show the pump intensity distributions before and after the geometric transformation components while the pump array is operating below the lasing threshold. Each bright spot in the first picture is the light emitted from a single subarray; the images of the 10 individual lasers constituting each subarray are unresolved. Correspondingly, each illuminated horizontal segment of the second photograph is the 50× image of a single, 10-laser subarray. The irregular vertical spacing of these horizontal segments is due to pump array facet curvature, as described below. The dark region in one segment in the lower left corner is the image of a single laser that evidently is defective.

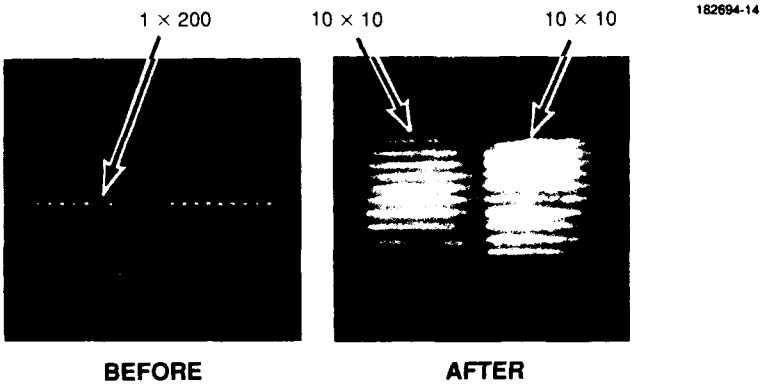

Figure 8. Photographs of the light patterns before and after the geometric transformation optics. On the left is a 1×200 *array of lasers and on the right are two symmetric sets of* 10×10 *lasers.*

Figure 9 shows the pump light distribution in the focal plane of the mode-matching lens along with lateral and transverse scans taken with a linear CCD camera through the focal spot. While the lateral scan shows a profile only approximately Gaussian in shape, the $1/e^2$ spot size of 57 μm corresponds to the diffraction-limited image of an individual emitter of the pump array. The transverse scan reveals a profile characterized by a similar $1/e^2$ spot size but also shows a tail and a discrete secondary feature on the lower side of the spot. These additional features are images of subarrays that have been incorrectly steered through the geometric transformation system because of uncompensated curvature of the pump array facet. The measured facet curvature is shown in Figure 10; newer versions of this array have significantly less curvature. As shown previously, a facet distortion of 5 μm from the average emitter position leads to a beam shift of 265 μm at the

second plane of microoptics and an angular deviation of approximately 10 mrad. Again, this shift could be accommodated by making the second array of lenses larger in the transverse direction. The photograph in Figure 9 shows the far-field intensity pattern of the pump beam. This pattern was also observed on a wall 6 m away when the focusing lens was removed.

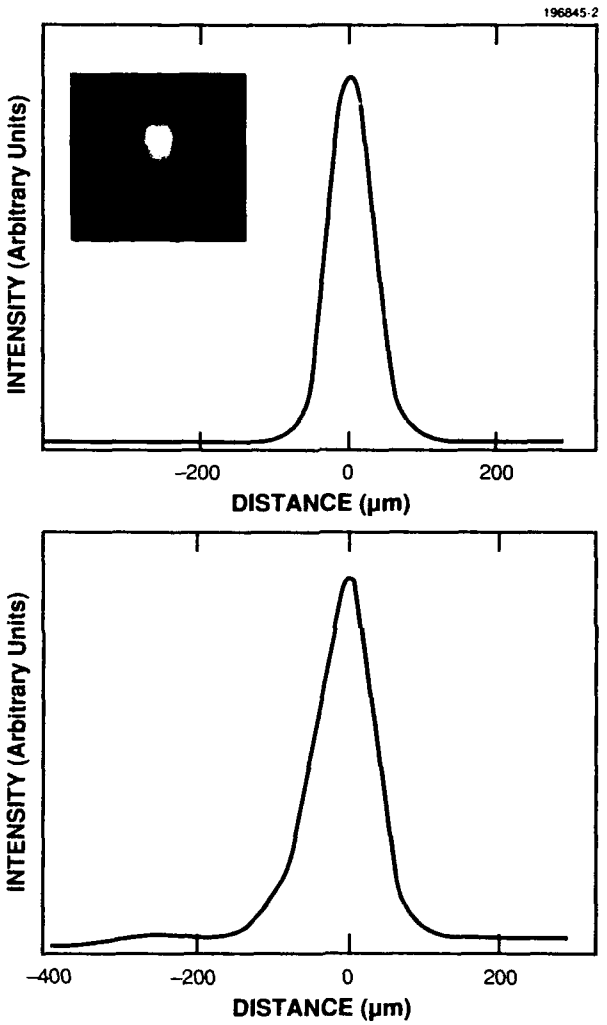

Figure 9. Photograph of pump spot at the lens focal plane. Upper trace shows a horizontal scan through the spot and lower trace is a vertical scan. Asymmetry of the vertical scan is due to curvature of the laser-diode array emitting facet.

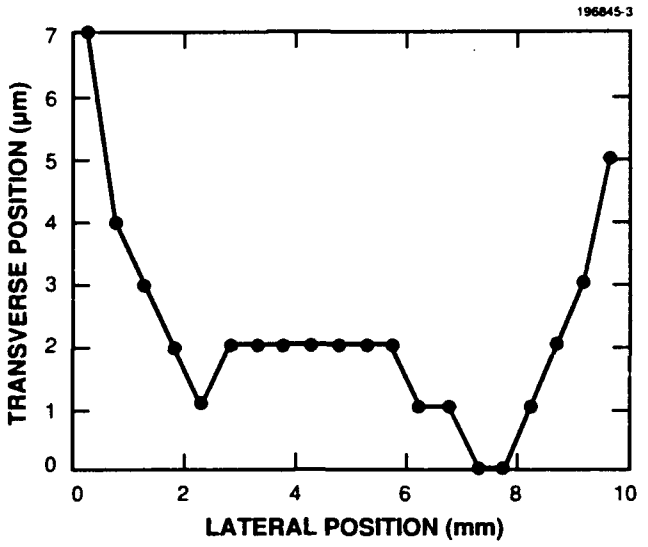

Figure 10. Curvature of the laser-diode array emitting facet as measured with an optical microscope.

The beam divergence ($1/e^2$ point) measured from Figure 9, exclusive of errant beams, is 1.5 mrad. Noting that the power through the transformation optics was 1.1 W and the emerging beam cross sectional area was 0.25 cm^2, the estimated average radiance of this source B' was 0.62 MW/cm^2 Sr. While the average CW intensity at the focus of our weakly converging pump beam was 10.8 kW/cm^2 (NA = 0.09 measured from the diagonal of the square pump array), an intensity exceeding 270 kW/cm^2 can be achieved with F/1 focusing optics.

Experimental results for the performance of the Nd:YAG laser are shown in Figure 11. Incident power upon the crystal has been corrected for the residual reflectivity of the facet coating. The laser operated in the TEM_{00} mode, as verified by analysis of the far-field diffraction pattern, at all incident power levels without the use of intracavity mode selection optics. The maximum CW output power of 480 mW was obtained with an incident power of 1.02 W for a peak efficiency of 47 percent. The optical slope efficiency from this plot is 56 percent. A slope efficiency of this magnitude is expected only if the mode overlap between the pump beams and the resonator mode is very good. The fact that Figure 9 shows a portion of the pump beam focused outside of the laser mode suggests that slope efficiencies could be improved by compensating for, or eliminating, the pump facet curvature.

The incident power on the crystal facet, 1.02 W, represents 19 percent of the total power emitted from the pump array. While a portion of our losses are due to Fresnel reflections from the uncoated diffractive optics and focusing lens, significant losses are directly attributable to the diffraction efficiency of the geometric transformation components. The diffraction efficiency of the

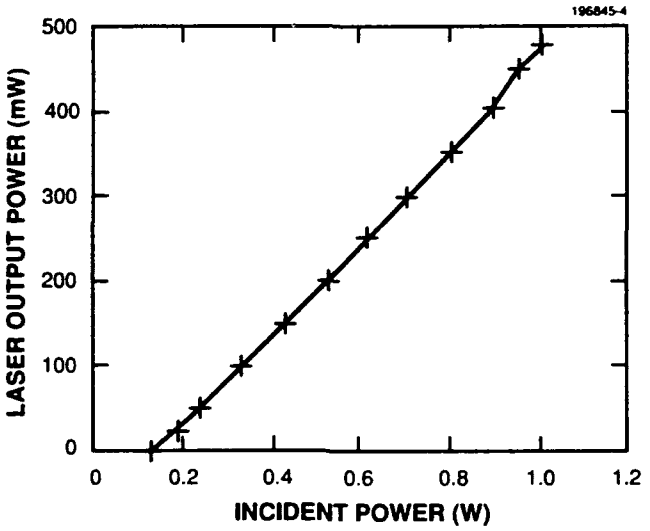

Figure 11. TEM_{00} output power from 1.06 μm transition of Nd:YAG crystal vs incident power from the geometrically transformed laser-diode array.

two components together was measured to be 25 percent, suggesting 50 percent per element. This low diffraction efficiency is not surprising because the numerical apertures of the elements is very high, and the substrate index (n = 1.45 for fused silica) is low. Higher efficiencies could be achieved by using a substrate with a higher refractive index.

Because all emitters of the SDL3480 were connected in electrical parallel, it was not possible to check the slope efficiency of the Nd:YAG laser under excitation by individual subarrays. However, by inserting a movable opaque mask between the pump array and the first microlens array, the incident pump power was increased by the contribution of one subarray at a time. Figure 12 shows the laser output power as the pump power is increased in this way. The data points represent the laser output power resulting from the integrated pump power from n subarrays as n increases from 1 to 20 while the horizontal separation between adjacent points shows the pump power contribution from the nth subarray. This plot shows a large variation in the emitted power from individual subarrays. More importantly, the lack of significant variation of the slope efficiency above threshold and the similarity of threshold powers here and in Figure 11 show that all subarrays are coupled to the resonator mode nearly equally. In particular, subarrays at the extreme ends of the laser bar (separated by up to 1 cm) contribute to the TEM_{00} laser mode.

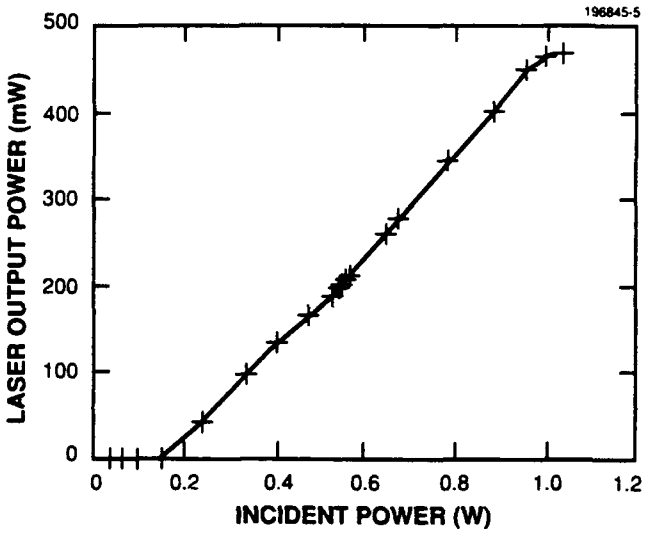

Figure 12. TEM_{00} output power from Nd:YAG laser when pumped by n subarrays ($1 \leq n \leq 20$) of the laser-diode array. Pump power emitted by the nth subarray is given by the difference between nth and nth − 1 abscissas.

7. THRESHOLD POWER MODEL

The expected threshold power for a laser of TEM_{00} mode radius ω_l, longitudinally pumped by a geometrically transformed laser-diode array, has been calculated. The threshold condition for lasing can be written in terms of an overlap integral I [12],

$$I = \int\int\int r_p(x,y,z)s_l(x,y,z)dv, \tag{25}$$

which accounts for the spatial overlap of the pump field r_p and resonator mode s_l. Because the pump field consists of a focused array of $M \times N$ individual beamlets, r_p and s_l take the following forms after normalizing each over the volume of the lasing medium:

$$\begin{aligned} r_p(x,y,z) &= \frac{2\alpha}{\pi {\omega_{p_0}}^2 [1-\exp(-\alpha L)]} \sum_{i=1}^{N}\sum_{j=1}^{M} \frac{{\omega_{p_0}}^2}{\omega_p(z-z_0)^2} \\ &\quad \times \exp\left(-2\frac{(x-x_i(z-z_0))^2+(y-y_j(z-z_0))^2}{\omega_p(z-z_0)^2} - \alpha z\right), \\ s_l(x,y,z) &= \frac{2}{\pi {\omega_l}^2 L}\exp\left(-2\frac{x^2+y^2}{{\omega_l}^2}\right) \end{aligned} \tag{26}$$

where α is the absorption coefficient, L is the crystal length, and $x_i(z)$ and $y_j(z)$ account for the off-axis propagation of the pump beams, each intersecting the optic axis at point z_0 inside the crystal. This discussion assumes that each pump beam of our symmetrized source is a circular Gaussian, propagating like

$$\omega_p(z) = \omega_{p_0}\sqrt{1+\left(\frac{\lambda z}{\pi n {\omega_{p_0}}^2}\right)^2} \tag{27}$$

despite oblique incidence of the beams upon a high index interface; for our typical experimental parameters, the beams acquire a negligible eccentricity of 0.08. In general, noncentrosymmetric beams can be described, as above, by a suitable substitution for $\omega_p(z)$ [13]. Following integration over x and y, Equation (25) becomes

$$\begin{aligned} I &= \frac{2\alpha}{NM\pi L[1-\exp(-\alpha L)]} \times \\ &\quad \sum_{i=1}^{N}\sum_{j=1}^{M}\int_0^L \frac{1}{{\omega_l}^2+\omega_p(z-z_0)^2}\exp\left(\frac{-2R_{i,j}(z-z_0)^2}{{\omega_l}^2+\omega_p(z-z_0)^2} - \alpha z\right)dz, \end{aligned} \tag{28}$$

where $R_{i,j}(z)^2 = x_i(z)^2 + y_j(z)^2$ is the radial displacement of the i,jth pump beam from the optic axis within the crystal. Simple focusing of the pump beams by a lens with focal length f results in a small-angle-approximation expression for $R_{i,j}(z)$ of

$$R_{i,j}(z) = \frac{z\sqrt{{x_{0_i}}^2 + {y_{0_j}}^2}}{n\sqrt{{x_{0_i}}^2 + {y_{0_j}}^2 + f^2}}, \tag{29}$$

where (x_{0_i}, y_{0_j}) is the position, relative to the optic axis, of the i,jth pump beam within the geometrically transformed source array before the focusing lens. By considering polarization and symmetry, the summations of Equation (28) need include only one quadrant of the transformed source array (i.e., $i,j = 1,5$). Finally, the diffraction-limited spot size of the individual Gaussian pump beams focused by a lens of focal length f in air is approximated by

$$\omega_{p0} = \frac{2\lambda f}{\eta\pi d}, \tag{30}$$

where d is the spacing of the geometrically transformed pump beams and η is the fill factor defined as the ratio between the Gaussian spot diameter and the pump-beam spacing. Equation (28), and therefore the threshold power, can be solved numerically with f and z_0 as parameters. The graphical solution for z_0 at minimum threshold power is used as an input parameter for generating the threshold power as a function of f and vice versa in an iterative fashion until the stationary points are found. The graphs of Figures 13 and 14 show the threshold power vs f and z_0 using the following parameters: an upper state lifetime of 2.3×10^{-4} s, a cross section of 3.2×10^{-19} cm^2, a pump quantum efficiency of 0.7, a scatter loss of 0.01 cm^{-1}, an output coupler transmission of 5 percent, an absorption coefficient of 4 cm^{-1} at 808 nm, a resonator mode radius of 210 μm, a lenslet diameter of 500 μm, a fill factor of 0.68, and a crystal length of 1 cm. The experimental results of Figure 11 agree with the expected optimization threshold power of Figure 13. For a similar treatment of the threshold power of fiber-coupled solid-state lasers, see Berger et al. [14].

The curve of Figure 13 is explained by noting that propagation of the pump beams is controlled by diffraction of the individual beams as well as the numerical aperture of the beam as a whole. For short focal lengths or high numerical aperture, the propagation angles of the beams relative to the optic axis are too large for good overlap with the resonator mode. Conversely, for large focal lengths, the diffraction-limited spot size of the individual beams given by Equation (30) is too large and causes a reduction of the mode overlap. Minimum threshold power is expected when these two effects are balanced.

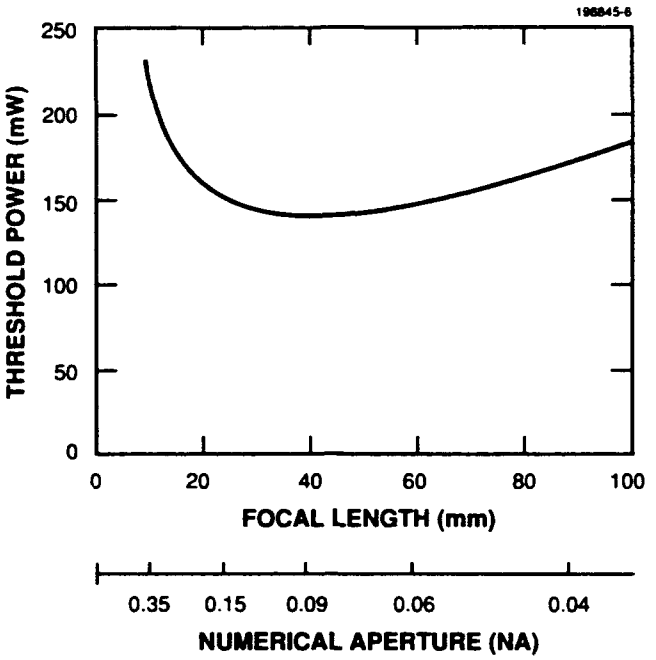

Figure 13. Calculated threshold power as a function of focal length of the pump-beam focusing lens using Equation (28).

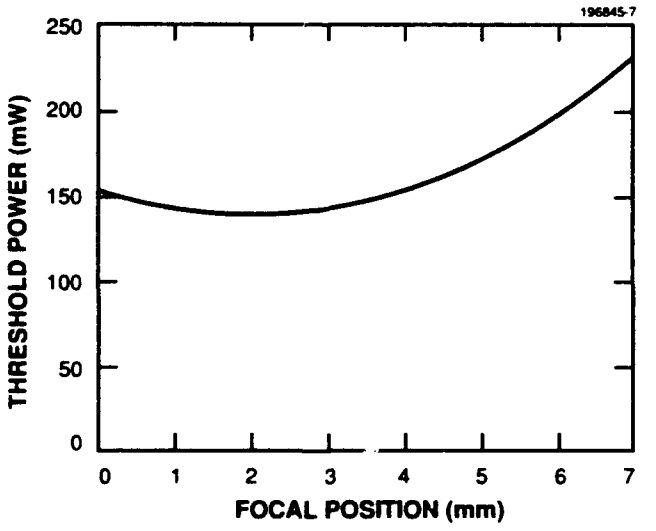

Figure 14. Calculated threshold power as a function of pump-beam focus position in lasing crystal from the crystal face.

8. ANALYSIS

While Equation (28) can be used to predict the threshold power for the fundamental mode, it does not indicate how many pump beams can be used to selectively excite the fundamental mode. In fact, this expression alone permits an indefinite number of pump beams. As the propagation angle of a pump beam increases, however, the absorbed power from this beam contributes increasingly to higher-order resonator modes. At some finite number of pump beams, higher-order modes in the resonator are expected.

In order to ensure lasing in the fundamental mode only, a modified version of Equation (18) can be used to estimate the number of pump beams (N) that contribute to this mode:

$$N = \frac{\pi^2 n^2 \eta_x \eta_y \omega_l^4}{2L^2 \lambda_p^2}, \tag{31}$$

where fill factors have been included in the lateral (η_x) and transverse (η_y) directions to account for less-than-perfect packing of the pump beams. Because this expression does not fully account for absorption of the pump beams, it only provides a lower limit estimate of the number of beams. Using the values from our experiment of $n = 1.8$, $\eta_x = \eta_y = 0.68$, $\omega_l = 210$ μm and $L = 6$ mm (90 percent of the power absorbed), Equation (31) predicts a capacity of 612 pump beams. This value is well above the 200 pump beams used in this experiment, so virtually all the pump power must be deposited within the fundamental mode volume, and higher order modes are not expected. If a fill factor of unity can be achieved, the pump beam capacity of this laser mode increases to 1,323 pump beams.

The étendue of the geometrically transformed pump beam was 1.77×10^{-6}cm^{2}Sr. The smallest étendue possible for 200 pump beams (polarization multiplexed) is 6.5×10^{-7}cm^{2}Sr or only 2.7 times smaller. The slightly larger experimental étendue can be accounted for by the suboptimal packing of Gaussian beams in the rectangular array.

The maximum average radiance B' is limited by the radiance theorem to that of two orthogonally polarized pump beams. Because each pump beam is Gaussian with an average power of 27.5 mW, the average radiance of a single pump beam B' is given by Equation (4) and the radiance from two cross-polarized pumps is 8.4 MW/cm^{2}Sr. The achieved value of 0.62 MW/cm^{2}Sr is 13.5 times smaller. The overall efficiency of the optics reduced the radiance by a factor of 5. The additional factor of 2.7 is a result of the slightly larger étendue.

The efficiency of the optics can be improved substantially by several methods. First, the efficiency of large-numerical-aperture diffractive optics can be increased by using a substrate with a high index of refraction. The substrate used in this experiment was fused silica ($n = 1.45$). Substrates with $n > 3$ will increase the efficiency considerably. The second method is to decrease the numerical aperture of the light presented to the diffractive optics. A pump array designed

with a larger transverse aperture will reduce the divergence and hence the numerical aperture requirements. Alternatively, the numerical aperture of the pump array can be reduced by a simple refractive cylindrical lens (such as a fiber lens [15]) placed between the array and the geometric transformation optics. Known aberrations introduced by the cylindrical lens can subsequently be removed by the diffractive optical elements. In addition, all the optics should be AR-coated to prevent Fresnel reflection losses. These changes should result in radiance levels that are close to the theoretical limits.

To compare alternative optical coupling methods to pump the laser in this experiment, consider using conventional macroscopic optics (cylindrical and spherical lenses, and anamorphic prism pairs). The total number of pump beams from a linear array M that can be coupled into the laser pump volume is given by a one-dimensional version of Equation (31):

$$N = \frac{\pi n \eta_x \omega_l^2}{L \lambda_p}. \tag{32}$$

The pump lasers in the SDL3480 are grouped together in subarrays spaced by large gaps, and this equation cannot be used directly to calculate N. If it is assumed that the fill factor η_x is unity and all other values are as previously given, Equation (32) gives a value of approximately 50 pump beams. Because this equation counts both polarizations, there is space for only 25 closely-packed pump beams. A single subarray of 10 pumps can occupy the first 10 locations. However, the geometry of the SDL3480 places the next 10-laser subarray 40 laser spacings away. Hence, only a single subarray (of each polarization) can be coupled into the fundamental mode, for a total of 20 pump beams. This result can be compared with the 612 pump beams possible with the microoptical system of this report.

A second method of coupling the pump beams into a laser rod uses a fiber bundle [14]. Each multimode fiber is butt-coupled to a single subarray, and the outputs of the fibers are collected into a two-dimensional bundle. The analysis starts by considering the problem of coupling one subarray into a multimode fiber by butt coupling. Assume for simplicity that the subarray fill factor is unity; the fiber core radius a must then be

$$a = \omega_p M \tag{33}$$

to accept M pump beams, where ω_p is the pump waist. Because the divergence of the pump given by Equation (1) cannot be greater than the numerical aperture of the fiber, there is a maximum number of single-polarization pump beams from a linear subarray given by

$$M = \frac{a\pi(NA)}{\lambda} = \frac{V}{2}, \tag{34}$$

where V is the V-number of the fiber. Because the theoretical maximum number of pumps [Equation (7)] is given by $V^2/2$, butt coupling to a linear laser subarray reduces the potential étendue and radiance by a factor of V. For example, the radiance from a butt-coupled multimode fiber with $NA = 0.3$ and core radius $a = 50$ μm is 116 times smaller than the theoretical maximum achievable with geometrical transformation.

Despite these inefficiencies, fibers have been used effectively to couple light from a linear pump array to a laser rod. The gaps in the pump array can be eliminated by choosing fiber cores that match the size of an individual laser subarray, and the fibers can be formed into a two-dimensional bundle to perform a geometric transformation. The principal radiance loss comes from coupling a single-linear subarray into a two-dimensional fiber core, as described above. One design [16] uses a fiber bundle to convert a linear array of pump lasers into a 380 μm-diameter aperture with a numerical aperture of 0.4. The étendue of the fiber bundle is 5.7×10^{-4} cm^{2}Sr or 320 times larger than the microoptics approach. Assuming the same total array power of 5.5 W used in this experiment and a fiber coupling efficiency of 80 percent, the radiance of the fiber-coupled system is 7.8 kW/cm^{2}Sr. This value is 80 times smaller than the radiance achieved by the present microoptics. The majority of the radiance reduction comes from coupling the linear laser subarray into the fiber.

It is interesting to compare the fiber-coupled laser array with its microoptics counterpart for rod laser pumping applications. First, apply the fiber-based system directly to pump the Nd:YAG laser described in the experimental section. The number of pump beams contributing to the fundamental laser mode can be calculated by comparing the laser étendue E_l to the étendue of the fiber bundle E_b. In this experiment, the laser mode waist $\omega_l = 210$ μm and E_l from Equation (17) is 1.33×10^{-6} cm^{2}Sr. E_b in the higher index of the laser rod is 1.75×10^{-4} cm^{2}Sr. Thus, only approximately 1 percent or 2 pump beams couple into the fundamental mode. Because of its larger étendue, the fiber-coupled pump requires a larger laser-mode waist with a corresponding higher threshold. The size of the required mode to contain all the pump beams from the fiber system can be estimated by equating E_b to E_l and solving for the laser mode waist ω_l:

$$\omega_l = \sqrt{\frac{2L}{\pi}} (E_b)^{1/4} = 711 \ \mu\text{m}. \tag{35}$$

The microoptics system of this report has an étendue in the crystal of 5.45×10^{-7} cm^{2}Sr, resulting in a minimum laser waist of 168 μm. Because lasing threshold is proportional to the square of the laser-mode waist, the microoptics approach reduces the theoretical threshold power by more than an order of magnitude.

As a final comparison, consider pumping the fiber laser described in Section 2.2 using conventional optics. The 45×110 μm rectangular inner cladding had a numerical aperture of 0.4. Assuming a 100 percent fill factor linear array oriented in the 110 μm direction, Equation (34) predicts the maximum number of pump beams $M = 86$ (where a is the half-width of the inner

cladding pump region). This corresponds to a total pump power of 5.6 W using pump beams of 65 mW each. Thermal constraints of CW arrays often require a reduced fill factor, resulting in even lower total pump powers. A comparison between this conventional optics limit and the 7,775 pump beams and over 500 W predicted in Section 2.2 dramatically demonstrates the power of the optical technique described in this report.

9. CONCLUSION

The fundamental radiance limits have been calculated for a mutually incoherent array of pump beams. An optical element was designed and fabricated to convert a linear pump array of 200 emitters into a two-dimensional source with maximum radiance and symmetrized shape and divergence. Testing of the element shows that the étendue achieved is within a factor of three of the theoretical limit. Further refinements to the fill factor and efficiency of the optics should achieve radiance levels that are essentially limited only by the radiance theorem. The optical element was used to longitudinally pump an Nd:YAG laser rod. The laser operated in a pure TEM_{00} mode with a slope efficiency of 56 percent.

The high radiance levels produced by these optics are especially significant for low-gain lasers, quasi-three-level lasers and double-clad fiber lasers where it is essential to concentrate the pump power into a small cross-sectional area with low beam divergence. Calculations show that the number of pump beams in some of these systems can be increased by several orders of magnitude when using these optics instead of conventional macroscopic and fiber-optic coupling schemes. The optical configuration contains several practical features as well. A single two-sided element can be designed to replace the conventional train of collimating lenses, anamorphic prism pairs, and focusing lenses. Alternatively, if an external focusing lens is employed, its off-axis performance requirements are significantly reduced by the aperture filling and geometrical transformation performed by the microoptics. In addition, this report showed that the microoptics can be designed to accommodate the mechanical tolerance requirements of virtually any laser system.

Although this report has concentrated on a specific geometrical transform for converting a line source into a uniformly filled circular or square one, the optical technique described is capable of transforming virtually any distribution of light into any other distribution (provided that the radiance theorem is not violated). In particular, light from wide stripe lasers, two-dimensional surface emitting lasers, and stacked laser arrays can be converted into other shapes and distributions. Finally, the technique can be applied to nonlaser-based light distributions such as those generated from incoherent light sources and conventional optical instruments.

REFERENCES

1. T.Y. Fan, "Efficient coupling of multiple diode laser arrays to an optical fiber by geometric multiplexing," *Appl. Opt. 30*, 630-632 (1991).
2. R.W. Boyd, *Radiometry and the Detection of Optical Radiation*, New York: Wiley (1983).
3. D. Botez and D.E. Ackley, "Phase-locked arrays of semiconductor diode lasers," *IEEE Circ. and Dev. 2*, 8-17 (1986).
4. J.R. Leger and M.P. Griswold, "Binary-optics miniature Talbot cavities for laser beam addition," *Appl. Phys. Lett. 56*, 4-6 (1990).
5. D. Gloge, "Weakly guiding fibers," *Appl. Opt. 10*, 2252-2258 (1971).
6. E. Snitzer, H. Po, F. Hakimi, R. Tumminelli, and B.C. McCollum, "Double clad, offset core Nd fiber laser," *Optical Fiber Sensors '88*, PD5, New Orleans (1988).
7. H. Po et al., paper PD-07, presented at the 1989 Optical Fiber Communication Conf., Houston, Texas (1989).
8. T.Y. Fan and A. Sanchez,"Pump source requirements for end-pumped lasers," *IEEE J. Quantum Electron. 26* 311-316 (1990).
9. T.Y. Fan, A. Sanchez, and W.E. DeFeo, "Scalable, end-pumped, diode-laser-pumped laser," *Opt. Lett. 14*, 1057-1059 (1989).
10. J.R. Leger, M.L. Scott, P. Bundman, and M.P Griswold, "Astigmatic wavefront correction of a gain-guided laser diode array using Anamorphic diffractive microlenses," *Proc. SPIE*, Vol. 884, 82-89 (1988).
11. G.J. Swanson, "Binary optics technology: theoretical limits on the diffraction efficiency of multilevel diffractive optical elements," MIT Lincoln Laboratory, Lexington, Mass., Technical Rep. 914 (1 March 1991), DTIC AD-A235404.
12. T.Y. Fan and R.L. Byer, "Diode Laser-Pumped Solid-State Lasers," *IEEE J. Quantum Electron. 24*, 895-912 (1988).
13. T. Brabec, F. Krausz, E. Wintner and A.J. Schmidt, "Longitudinal pumping of lasers with multistripe laser diodes," *Appl. Opt. 30*, 1450-1454 (1991).
14. J. Berger, D.F. Welch, W. Streifer, D.R. Scifres, N.J. Hoffman, J.J. Smith, and D.Radecki, "Fiber-bundle coupled, diode end-pumped Nd:YAG laser," *Opt. Lett. 13*, 306-308 (1988).
15. T.M. Baer, D.F. Head, and M. Sakamoto, "High efficiency diode-bar pumped solid-state laser using a tightly folded resonator," *Conf. on Lasers and Electro-optics: Digest of Technical papers*, Optical Society of America, p. 416 (1989).
16. Spectra Diode Labs 1991 Product Catalog, model SDL3450-P5.

REPORT DOCUMENTATION PAGE

Form Approved
OMB No. 0704-0188

1. AGENCY USE ONLY (*Leave blank*)	2. REPORT DATE	3. REPORT TYPE AND DATES COVERED
	26 May 1992	Technical Report

4. TITLE AND SUBTITLE
Geometrical Transformation of Linear Diode-Laser Arrays for Longitudinal Pumping of Solid-State Lasers

5. FUNDING NUMBERS
C — F19628-90-C-0002
PE — 62702E
PR — 305

6. AUTHOR(S)
James R. Leger and William C. Goltsos

7. PERFORMING ORGANIZATION NAME(S) AND ADDRESS(ES)
Lincoln Laboratory, MIT
P.O. Box 73
Lexington, MA 02173-9108

8. PERFORMING ORGANIZATION REPORT NUMBER
TR-950

9. SPONSORING/MONITORING AGENCY NAME(S) AND ADDRESS(ES)
DARPA
1400 Wilson Blvd.
Arlington, VA 22209-2308

10. SPONSORING/MONITORING AGENCY REPORT NUMBER
ESD-TR-91-250

11. SUPPLEMENTARY NOTES
None

12a. DISTRIBUTION/AVAILABILITY STATEMENT
Approved for public release; distribution is unlimited.

12b. DISTRIBUTION CODE

13. ABSTRACT (*Maximum 200 words*)

A 200-stripe linear diode-laser array is geometrically transformed into a two-dimensional, symmetric virtual source with symmetric divergence to end-pump a Nd:YAG laser. The geometrical transformation is performed by two planes of diffractive optical elements separated by a 2.6-cm gap. Discounting optical losses, a TEM_{00}-mode slope efficiency of 56 percent is demonstrated. Methods of increasing the throughput efficiency of the diffractive elements (currently approximately 50 percent per element) are explored. A theoretical model for estimating the maximum useful pump array size in longitudinally pumped rod and fiber lasers shows that this pump geometry is close to optimum.

14. SUBJECT TERMS			15. NUMBER OF PAGES
solid-state lasers	binary optics	étendue	50
longitudinal pumping	microlens arrays	geometrical transformation	16. PRICE CODE
diffraction optics	microoptics		

17. SECURITY CLASSIFICATION OF REPORT	18. SECURITY CLASSIFICATION OF THIS PAGE	19. SECURITY CLASSIFICATION OF ABSTRACT	20. LIMITATION OF ABSTRACT
Unclassified	Unclassified	Unclassified	Unclassified